The Silicon Drift Detector for the IXO High Time Resolution Spectrometer

Peter Lechner*[a], Carine Amoros[b], Didier Barret[b], Pierre Bodin[c], Martin Boutelier[b], Rouven Eckhardt[a], Carlo Fiorini[d], Eckhard Kendziorra[e], Karine Lacombe[b], Adrian Niculae[a], Benjamin Pouilloux[c], Roger Pons[b], Damien Rambaud[b], Laurent Ravera[b], Christian Schmid[f], Heike Soltau[a], Lothar Strüder[gh], Christoph Tenzer[e], Jörn Wilms[f]

[a] PNSensor GmbH, Römerstr. 28, 80803 München, Germany;
[b] Centre d'Etude Spatiale des Rayonnements, 9 Av. du Colonel Roche, 31028 Toulouse, France;
[c] Centre National d'Etudes Spatiales, 18 Av. Edouard Belin, 31401 Toulouse, France;
[d] Politecnico di Milano, Dipartimento di Elettronica e Informazione, Via Golgi 40, 20133 Milan, Italy;
[e] Institut für Astronomie und Astrophysik, Sand 1, 72076 Tübingen, Germany;
[f] Dr. Remeis-Observatorium, Sternwartstr. 7, 96049 Bamberg, Germany;
[g] Max-Planck-Institut für extraterrestrische Physik, Giessenbachstr., 85741 Garching, Germany;
[h] MPI Halbleiterlabor, Otto-Hahn-Ring 6, 81739 München, Germany;

ABSTRACT

The High Time Resolution Spectrometer (HTRS) is one of six scientific payload instruments of the International X-ray Observatory (IXO). HTRS is dedicated to the physics of matter at extreme density and gravity and will observe the X-rays generated in the inner accretion flows around the most compact massive objects, i.e. black holes and neutron stars. The study of their timing signature and in addition the simultaneous spectroscopy of the gravitationally shifted and broadened iron line allows for probing general relativity in the strong field regime and understanding the inner structure of neutron stars. As the sources to be observed by HTRS are the brightest in the X-ray sky and the studies require good photon statistics the instrument design is driven by the capability to operate at extremely high count rates.

The HTRS instrument is based on a monolithic array of Silicon Drift Detectors (SDDs) with 31 cells in a circular envelope and a sensitive volume of 4.5 cm^2 x 450 µm. The SDD principle uses fast signal charge collection on an integrated amplifier by a focusing internal electrical field. It combines a large sensitive area and a small capacitance, thus facilitating good energy resolution and high count rate capability. The HTRS is specified to provide energy spectra with a resolution of 150 eV (FWHM at 6 keV) at high time resolution of 10 µsec and with high count rate capability up to a goal of $2 \cdot 10^6$ counts per second, corresponding to a 12 Crab equivalent source. As the HTRS is a non-imaging instrument and will target only point sources it is placed on axis but out of focus so that the spot is spread over the array of 31 SDD cells. The SDD array is logically organized in four independent 'quadrants', a dedicated 8-channel quadrant readout chip is in development.

Keywords: International X-ray Observatory, IXO, High Time Resolution Spectrometer, HTRS, X-ray Astronomy, X-ray Spectroscopy, X-ray Timing, Silicon Drift Detector, SDD

1. INTRODUCTION

The International X-ray Observatory (IXO) [1] is a joint high-energy mission of the US-American, European, and Japanese space agencies with a projected launch in 2021 to a large-amplitude halo orbit around the second Lagrange point (L2) of the sun-earth system. IXO will address some of the most fundamental questions in contemporary astrophysics and cosmology. Among the primary science goals are the investigation of black holes and matter under extreme conditions, the study of formation and evolution of galaxies, clusters and large scale structure, and to trace the life cycles of matter and energy. This variety of scientific tasks requires high sensitivity and high spatial resolution over a

* corresponding author, peter.lechner@pnsensor.de; phone +49.89.83940051; www.pnsensor.de; www.hll.mpg.de;

High Energy, Optical, and Infrared Detectors for Astronomy IV, edited by Andrew D. Holland, David A. Dorn
Proc. of SPIE Vol. 7742, 77420W · © 2010 SPIE · CCC code: 0277-786X/10/$18 · doi: 10.1117/12.857260

broad energy band with excellent energy and time resolution. Therefore, IXO combines a large aperture X-ray mirror with a set of complementary focal plane sensors. The light-weight X-ray optical system has a focal length of 20 m, a goal collecting area of 3 m², and an angular resolution of 5 arcsec. The instrument payload includes six specialized sensor systems:

- The X-ray Microcalorimeter Spectrometer (XMS) is based on a transition edge sensor and provides high spectral resolution (few eV), non-dispersive imaging spectroscopy in the 0.3-7.0 keV band.
- The Wide Field Imager (WFI) is an imaging X-ray spectrometer based on a Silicon active pixel sensor with a large field of view (~ 20 arcmin) and Fano-limited energy resolution (130 eV at 5.9 keV), covering the 0.1-15 keV band.
- The Hard X-ray Imager (HXI) is a Cadmium-Telluride double-sided strip detector located behind the WFI and observing simultaneously with it, extending the energy coverage up to 40 keV.
- The X-ray Grating Spectrometer (XGS) is a wavelength-dispersive spectrometer composed of diffraction gratings and a CCD camera that will provide high spectral resolution in the soft X-ray band (0.3-1.0 keV) with a resolving power $\lambda/\Delta\lambda$ of 3000.
- The High Time Resolution Spectrometer (HTRS) is a non-imaging instrument performing high precision timing and spectroscopy measurements of bright X-ray sources.
- The X-ray Polarimeter (XPol) is an imaging polarimeter, with polarization sensitivity of 1 % utilizing a fine grid gas pixel detector to image the tracks of photoelectrons produced by incident X-rays.

Five of the instruments (XMS, the combined WFI/HXI, HTRS, and XPol) are placed on a Moveable Instrument Platform (MIP) rotating the selected instrument into the focus. Science data will be collected using one of the MIP-mounted instruments at a time. The CCD camera of the XGS instrument is placed on the Fixed Instrument Platform and will operate simultaneously with the observing MIP instrument.

The High Time Resolution Spectrometer[♦] is the only focal plane instrument to match the IXO top level requirement to observe a bright X-ray source of the intensity of one Crab with less than 10 % dead time. The HTRS science will be focused on matter under extreme conditions, targeting galactic compact objects powered by accretion. It offers a complementary tool for probing strong gravity in the vicinity of accreting black holes and neutron stars and for probing matter at supra-nuclear densities by simultaneous fast X-ray timing and high-resolution spectroscopy measurements. As the sources to be observed by HTRS are the brightest in the X-ray sky and the studies require good photon statistics the instrument design is driven by the capability to operate at extremely high count rates. The only available sensor concept that is able to cope with the HTRS requirements summarized in table 1 is the Silicon Drift Detector (SDD). It combines a large sensitive area with an extremely small readout capacitance and is therefore predetermined for high-rate high-resolution X-ray spectroscopy. The HTRS instrument is designed around a monolithic array of 31 SDD cells. As HTRS is a non-imaging instrument and will target only point sources it is placed on axis but out of focus so that the intense photon flux is spread evenly over the array of 31 SDD cells.

Table 1. The sensor requirements of the IXO High Time Resolution Spectrometer. With the current concept of the IXO telescope the intensity of the Crab pulsar corresponds to approximately 170.000 photons per second.

energy range	0.3 - 15 keV	
time resolution	10 μsec	
energy resolution (-40 °C) FWHM @ 5.9 keV	150 eV ≤ 200 eV ≤ 300 eV	(goal at beginning of lifetime) (requirement at beginning of lifetime) (requirement at end of lifetime)
count rate capability	> 10 Crab	
deadtime & pile-up	< 2% @ 1 Crab	

♦ The companion paper D. Barret et al., "The High Time Resolution Spectrometer (HTRS) aboard the International X-ray Observatory (IXO)", also presented at the SPIE Conference Astronomical Telescopes and Instrumentation 2010, provides a general description of the HTRS including the science case and system aspects.

2. SILICON DRIFT DETECTOR

Silicon Drift Detectors (SDDs) are based on the principle of sideward depletion [2] a large volume of a high resistivity semiconductor, in our case n-type silicon, is depleted by a small sized n^+ bulk contact reverse biased with respect to rectifying p^+ junctions covering both surfaces of the structure. In an SDD the p^+ junctions are strip-like segmented and biased in such a way that an electric field parallel to the surface exists. Electrons released within the depleted volume by the absorption of ionizing radiation or by thermal generation drift in the field towards the n^+ substrate contact, which acts as collecting anode and is connected to an amplifier. The generated holes are drained away by the p^+ junctions.

Originally SDDs have been proposed as position sensitive detectors in particle physics where the measurement of the signal electrons' drift time allows reconstructing the particle's interaction point. In an advanced SDD design optimized for applications in photon spectroscopy the p^+ strip system for the generation of the drift field has the shape of concentric rings. The drift rings and the collecting anode in their center are placed on one side of the structure, while the opposite surface is covered by a non-structured p^+ junction acting as homogeneous radiation entrance window [3], [4] (figs. 1, 2). As the potentials of the field strips are defined by an integrated resistive voltage divider, only the first and the last ring must be biased externally. There is no field-free region in the device, and the whole volume is sensitive for the absorption of ionizing radiation. Each electron generated in the volume is collected at the anode in the center of the front side. The typical charge collection time is of the order of 100 nsec. SDDs of this type do not provide position information but are used as energy dispersive spectrometers, taking advantage of the small value of the anode capacitance, which is almost independent of the detector area. For a given number of collected electrons this quality translates to large amplitude and short rise time of the output signal. Compared to a photodiode of equal size and operated at the same conditions

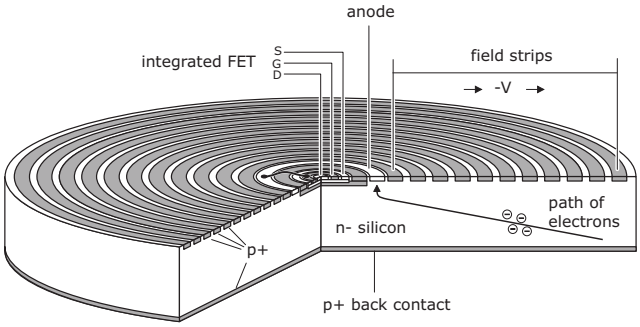

Figure 1. Schematic view of a cylindrical Silicon Drift Detector. Electrons are guided by a radial electric field towards the small sized collecting anode and the readout transistor in the center of the device.

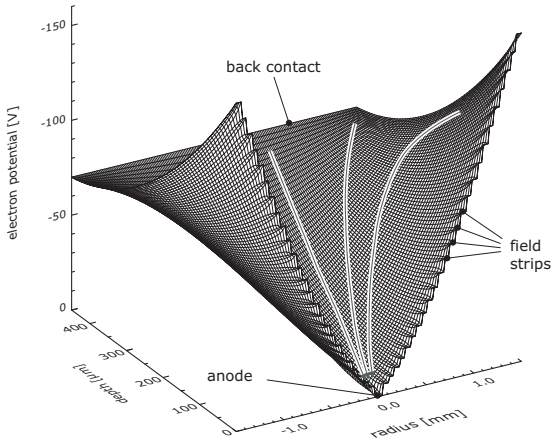

Figure 2. Calculated electron potential energy of an SDD device as shown in fig. 1 in a section through the anode perpendicular to the surface. In the back there is the constant potential of the entrance window, the field strips with their step-like increasing negative potential are visible in the front.

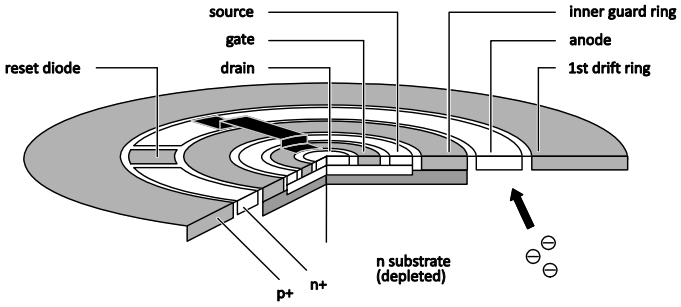

Figure 3. Section of the readout structure of an SDD as shown in fig. 1. Signal electrons are accumulated on the n^+-doped anode which is connected by a metal strip to the gate of the integrated first FET. To discharge the anode the reset diode is pulsed to forward bias.

(temperature, noise of readout electronics) the SDD is able to work at higher count rates and yields a substantially better energy resolution, because the signal is less sensitive to the noise contribution of the subsequent amplifying electronics.

The SDD's output capacitance is optimized by the device topology with the small dimension of the collecting anode. A further reduction and an additional gain in signal rise time and energy resolution can only be achieved by minimizing the remaining contributions: the amplifier's input capacitance and the stray capacitance of the connection between detector and amplifier. Both goals are achieved simultaneously by integrating the first transistor of the amplifying electronics on the SDD chip. The integrated transistor can be designed with minimum input capacitance, which is unusual for discrete devices, and the bond wire connecting detector and amplifier in the traditional setup is replaced by a short metal strip on the chip. That way the system also gets robust with respect to microphonic noise by mechanical vibrations and electrical pickup.

The integrated transistor is a single-sided n-channel JFET [5] placed inside the ring shaped anode in the center of the device (figs. 1, 3). Signal charges are collected on the n^+-doped anode which is connected to the FET gate by a metal strip. A p^+-doped reset diode is inserted in the anode. It is pulsed from reverse to forward bias to discharge the anode. Due to its minimized overall capacitance in the order of 100 fF the SDD with integrated transistor has its optimum noise figure at extremely short shaping time constants ≤ 1 µsec and it works at photon rates exceeding 10^5 cps (counts per second) without degradation in its spectroscopic performance (see fig. 11). The low leakage current level obtained by the elaborated process technology allows operating SDDs at room temperature or with moderate cooling, e.g. by a thermoelectric cooler.

SDDs of this type have been produced in large numbers and are available in a multitude of shapes and sizes from 5 mm² up to 1 cm². They are primarily used for X-ray spectroscopy in industrial instrumentation and scientific experiments. SDDs also have collected space experience in the Alpha Particle X-ray Spectrometers on the robotic arms of the NASA Mars Exploration Rovers *Spirit* and *Opportunity* [6].

To increase the sensitive area without loss in performance monolithic SDD arrays have been developed [7]. The largest multi-channel SDD in use is composed of 77 hexagonal cells each having a sensitive area of 8.7 mm² [8]. The SDD cells are arranged in a honeycomb structure with a fill factor of 100 % in an envelope of 29 x 26 mm².

3. SDD FOR THE HIGH TIME RESOLUTION SPECTROMETER

3.1 Layout

The HTRS sensor is a multi-channel SDD consisting of 31 cells in a circular envelope of 24 mm diameter and a total area of 4.5 cm². The central cell has a circular shape. The outer cells have the shape of ring sectors and are arranged in three rings of 1 x 6 and 2 x 12 cells (figs. 4, 5). All cells have equal areas of 14.6 mm². The thickness of the Silicon wafer is 450 µm. One surface of the sensor is filled with the integrated readout structures and the drift ring system defining the collecting electric field. The 31 SDD cells are logically grouped in four 'quadrants' of seven or eight cells, as

indicated in fig. 4. The quadrants are to a large extent electrically independent, including redundant supply and readout electronics. The readout structures of each quadrant's cells are connected to an eight-channel readout chip (section 3.3). For redundancy the center of the device is shared between the four quadrants, because only the central cells will receive hard energy X-rays.

For each sensor cell the surface opposite to the drift and readout structures is made of a shallow non-structured junction acting as thin homogeneous entrance window for backside illumination. The border lines between the cells' entrance windows will be masked by a laser cut absorbing baffle (fig. 6). The baffle inhibits split events caused by photons absorbed close to the cell border. Split events generate signal charges in two or more neighboring cells, which the HTRS readout and data processing electronics could not allocate and reconstruct. Therefore, split events would cause false energy information. A first set of 'spider web' shaped baffle prototypes made of 450 µm thick Silicon with 200 µm wide rings and spokes has been produced by laser cutting. The final version will be made of a better absorbing material. A baffle with 200 µm wide bars covers a 10 % fraction of the total sensitive area, but it increases the spectral quality as the sensor cells will always receive the full photon signal of single events.

For demonstration and for a structural and thermal model a mechanical sample of the HTRS sensor has been fabricated (fig. 5). It has the visible metal structures on both sides of the chip: on the front side the drift ring structures and the connections from the readout nodes to the quadrant-arranged bond pads, and on the back side the boundaries between the cells' entrance windows. The chip has the shape of a regular octagon with 11.6 mm side length and 28 mm diameter. A seven-cell prototype sensor with 7 x 10 mm² sensitive area representing the core part of the final HTRS device is currently in production.

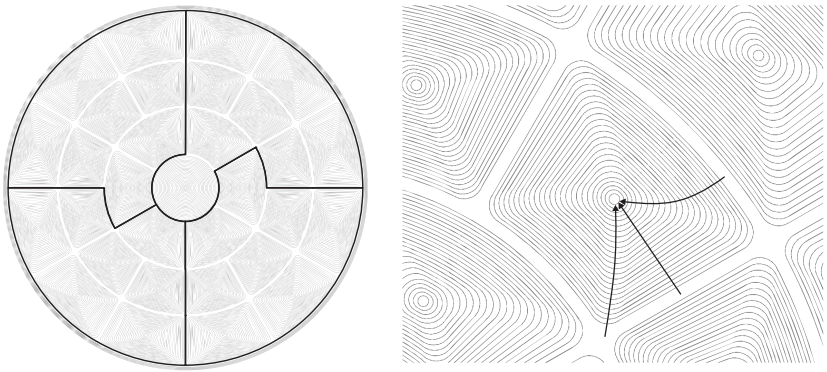

Figure 4. Layout of the 31-cell SDD for HTRS. Electrons drift perpendicular to the drift ring structures towards the readout structure in the cell center. The bold lines indicate the quadrant organization of the device. In the layout shown here the cell sizes vary with the radial position, the final design will have equal cell sizes.

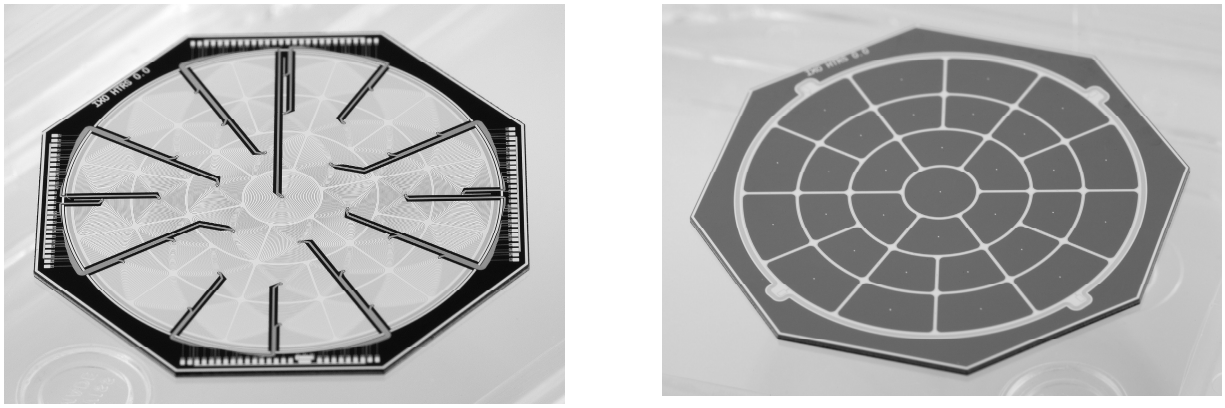

Figure 5. Mechanical sample of the HTRS sensor, readout side (left) and radiation entrance window side (right). In the layout shown here the cell sizes vary with the radial position, the final design will have equal cell sizes.

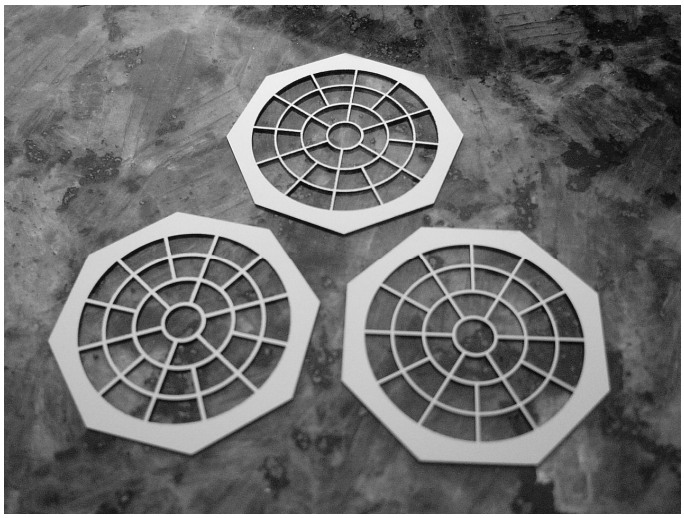

Figure 6. 'Spider Web' collimator test samples made by laser cutting of 450 µm Silicon with 400 µm (left), 300 µm (right) and 200 µm (back) width of the rings and spokes. The final collimator will be made of better absorbing material. In the layout shown here the cell sizes vary with the radial position, the final design will have equal cell sizes.

3.2 Performance

At the HTRS experimental conditions, i.e. sensor temperature -40 °C and short signal processing time for high count rate handling, the SDD energy resolution will be ≤ 150 eV FWHM at 5.9 keV at the beginning of the lifetime. The energy resolution is stable within 2 % and the gain variation is less than 2 ‰ even at count rates exceeding 10^5 photons per second and SDD cell, corresponding to a source intensity > 10 Crab (section 3.3, fig. 11). The SDD's quantum efficiency is above 90 % in the energy band from 0.5 to 10 keV (fig. 7). Photons at higher energies are transmitted through the finite Silicon thickness of 450 µm without interaction. At low energies the quantum efficiency is limited by the entrance window's Si dead layer and by a thin Al layer deposited on the window.

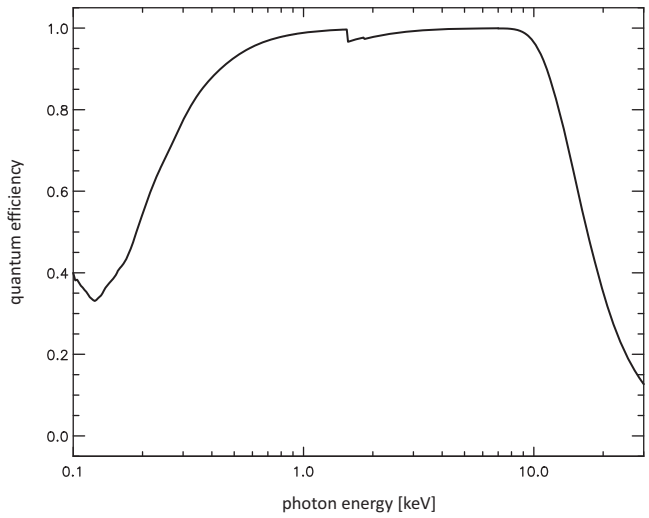

Figure 7. Calculated quantum efficiency of the SDD for HTRS. The quantum efficiency is > 90 % for energies from 0.5 to 10 keV. The drop-offs at high and low energy are caused by the entrance window's dead layer and by a thin Al layer covering the window and by the finite thickness of the Si bulk respectively.

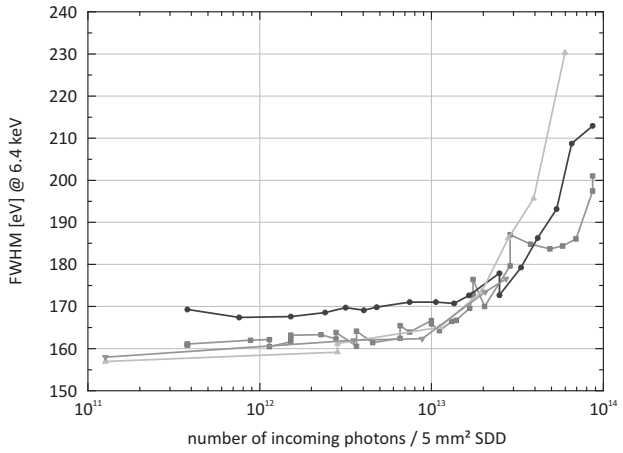

Figure 8. Radiation hardness measurement of four 5 mm² SDD samples with respect to X-rays. The energy resolution is not affected up to 10^{13} photons (Mo-K, 18 keV) absorbed in the 5 mm² sensitive area. This photon number exceeds the IXO-HTRS observation scenario by orders of magnitude.

SDDs processed in the technology that will be applied for the HTRS sensor have been proven to be radiation hard with respect to X-rays up to a number of 10^{13} absorbed photons (Mo-K, 18 keV) without degradation of the energy resolution (fig. 8). This figure would theoretically allow for a ten years continuous observation of a bright source with an intensity of several Crabs.

In addition to photon irradiation the HTRS sensor will be exposed to $2 \cdot 10^9$ ($5 \cdot 10^9$) protons (10 MeV equivalent) per cm² in a 5 (10) years mission, assuming an effective shielding represented by 15 mm of Aluminum. Protons create defects in the Silicon crystal lattice, which are generation centers for leakage current. Based on experimental data [9] this non-ionizing radiation effect has been modeled to cause an additional leakage current of $2.43 \cdot 10^{-17}$ A at room temperature per 10 MeV proton. The corresponding deterioration of the energy resolution is ≤ 250 eV FHWM at 5.9 keV towards the end of the mission lifetime (EOL), still meeting the system specifications within a sufficient margin (fig. 9).

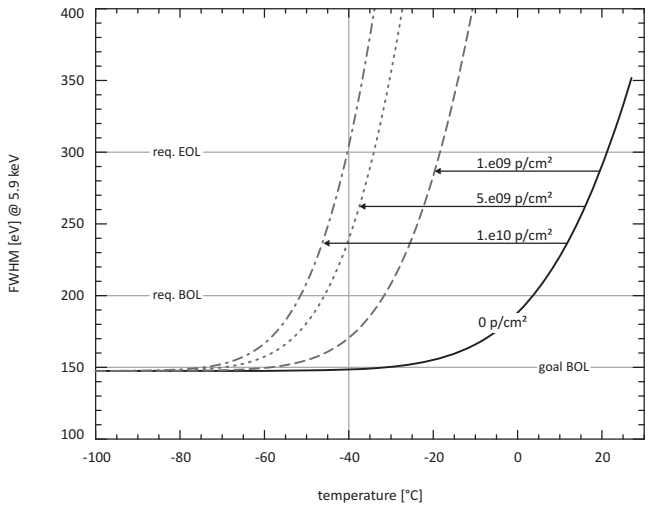

Figure 9. Modeled proton irradiation effect on the HTRS sensor. The energy resolution vs. temperature characteristics is shifted by the additional leakage current generated in proton-induced Si crystal defects. At the HTRS sensor temperature of -40 °C the calculated energy resolution will be ≤ 250 eV FHWM at 5.9 keV at the expected dose of $5 \cdot 10^9$ protons (10 MeV equivalent) per cm². This value still meets the requirement at the end of lifetime (EOL) within a sufficient margin.

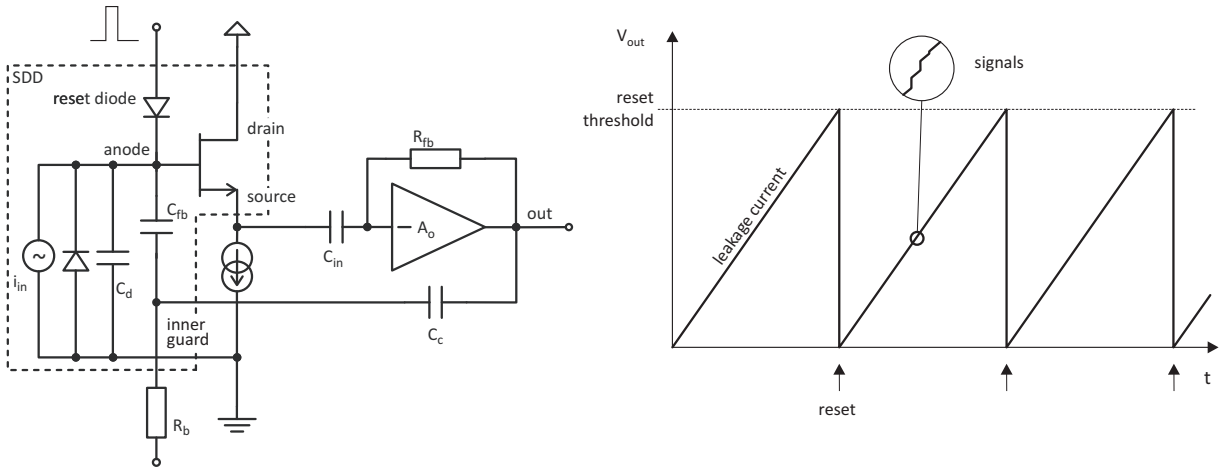

Figure 10. Charge sensitive amplifier configuration of the integrated FET (left) and SDD output signal (right).

3.3 Readout and data acquisition

The baseline for the signal amplifying electronics is a fully analog readout chain integrated in an 8-channel readout chip. The readout circuit provides pre-amplification and analog filtering of the SDD signals. The pre-amplifier operates with the first FET integrated on the SDD chip configured as a charge sensitive amplifier (CSA, fig. 10) [10]. For the capacitive feedback the parasitic capacitance of the reverse biased junction between the charge collecting anode and a guard ring is used, its value is about 30 … 35 fF. The leakage current and the signals are integrated on this feedback capacitance C_{fb} generating a voltage ramp with superposed steps at the pre-amplifier output (fig. 10). Whenever the output voltage exceeds a preset threshold value the readout chip produces a signal which is used to trigger an external reset circuit discharging the SDD. For this purpose a p^+-doped reset diode is integrated directly in the anode (fig. 3). The reset diode is reverse biased (-15 V) during signal integration and pulsed to forward bias (+7 V) for the reset. The duration of the reset pulse is 300 … 500 nsec. The reset signal is common for all eight channels of the readout chip, and so the average reset period is determined by the channel with the highest sum of leakage and signal currents.

The filter amplifier is a 9^{th} order semi-Gaussian shaper with two selectable amplification settings allowing for the processing of photons with a maximum energy of 10 keV and 20 keV. The filter function has a peaking time of 600 nsec corresponding to a pulse width of 1.2 µsec. The chosen filter time constant is a compromise between energy resolution, which would improve for longer time constants, and count rate capability. With 600 nsec peaking time the dead time is calculated to be about 1 % (10 %) at an input count rate of 10.000 (100.000) photons per second and sensor channel, while the energy resolution is 150 eV FWHM at 5.9 keV with the cell size and operating temperature of the HTRS.

The analog chain is completed by a baseline holder, an event trigger, a peak stretcher, and a fast shaper channel with a peaking time of 200 nsec for pile-up detection and rejection. The analog amplitudes of the eight channels together with the channel addresses are delivered to an external analog/digital converter (ADC) by an 8/1 analog multiplexer operating at 10 MHz. The design of a prototype of the analog eight-channel readout chip has been completed. It will be submitted for fabrication in the AMS 0.35 µm technology in July 2010.

The analog readout configuration with CSA and pulsed reset has been tested using a 5 mm² SDD and conventional discrete components for the electronic chain. The spectroscopy performance is almost independent of the input count rate up to 10^5 cps: the energy resolution (FWHM at 5.9 keV) is stable on the 1 % level and the peak position is stable on the 0.1 % level (fig. 11).

As an alternative readout strategy to the analog chip a digital readout chain is under study. In the digital option the configuration and operation mode of the integrated first FET is unchanged. The readout chip includes eight pre-amplifiers only. The pre-amplifier output signals of each channel are sampled by a fast (150 MHz) 14 bit ADC and filtered by software filter functions with effective time constants comparable to the analog shaper: 200 nsec for event detection and 600 nsec for the precise measurement of the signal amplitude. The digital option is of great flexibility, as

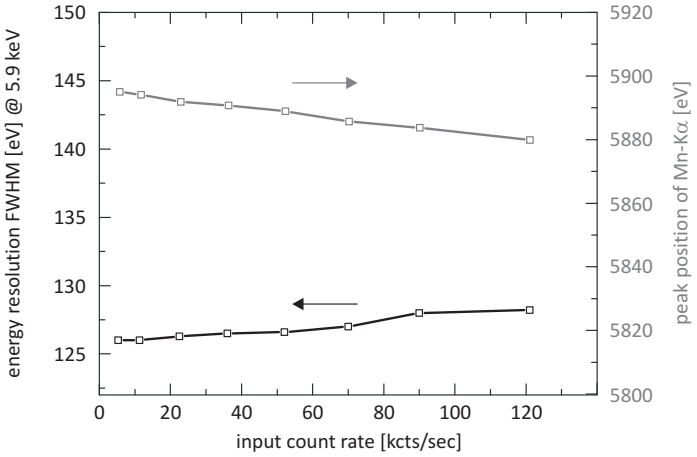

Figure 11. Measured high rate performance of a 5 mm² SDD with integrated FET in CSA-configuration and pulsed reset. The energy resolution in terms of FWHM at 5.9 keV and the peak position are stable with count rate on the 1 % and 0.1 % level respectively [10].

its function is mainly based on software which can be developed and adapted even after the launch. On the other hand it requires one fast ADC per sensor channel and has a higher power budget than the analog readout. A more detailed tradeoff analysis of the analog and digital readout options is discussed in the companion paper mentioned in section 1.

In the downstream Data Processing Unit (DPU) the digitized events get a time tag and a cell-individual gain correction before they are binned to energy spectra in time slices of <10 μsec. The HTRS will produce a high data rate. To stay within the telemetry limits as allocated by ESA during the assessment phase, a number of data rate saving measures is under study: efficient data compression algorithms, an on-board mass memory as a temporary storage for peak data accumulation, and an elaborated observation plan foreseeing alternating bright and faint source targets.

3.4 Focal Plane arrangement

The thermal, mechanical and electrical interface to the HTRS sensor is given by the sensor hybrid. To keep the quadrant philosophy an individual hybrid is assigned to each sensor quadrant. The four hybrids are glued on a common ceramic base frame. The sensor hybrids contain passive RC-components for supply voltage filtering. Per quadrant there is one power flex-lead connected to the electronics box and carrying the sensor supply voltages and one signal flex-lead connected to the readout board and including the signal, feedback and trigger lines. The sensor chip and the flex-leads are electrically connected to the hybrid by wire bonding. To keep the setup compact the active components of the readout electronics are placed on a separate readout board behind the sensor hybrid. To minimize the X-ray fluorescence radiation seen by the sensor a graded shield plate is inserted between the sensor hybrid and the readout board. Both the sensor hybrid and the readout board are enclosed by an Aluminum box acting both as radiation shield and thermal interface (fig. 12).

As HTRS is a non-imaging instrument operating at high count rates the sensor is displaced from the focal plane to distribute the photon flux homogeneously over the 31 SDD cells. The out-of-focus distance is chosen such that with the given SDD format 99.9 % of the incoming photons fall into the sensor radius even in the worst case misalignment scenario: 1 mm shift out of the nominal position in all three directions, 2 ° sensor tilt, 5 arcsec off-axis pointing. With the actual mirror design (3 m² at 1.25 keV) the out-of-focus distance is 11.3 cm.

The sensor assembly is mounted thermally decoupled on the filter wheel support structure. The sensor is cooled through the Al housing to its nominal temperature -40 °C. The filter wheel protects the sensor with respect to contamination and optical load. It has five positions: open, closed, thin filter (30 nm Al), thick filter (50 nm Al), and calibration equipped with a ^{55}Fe/Al fluorescence source producing the Mn-K lines at 5.9 keV and 6.4 keV and the Al-K line at 1.5 keV for in-flight calibration.

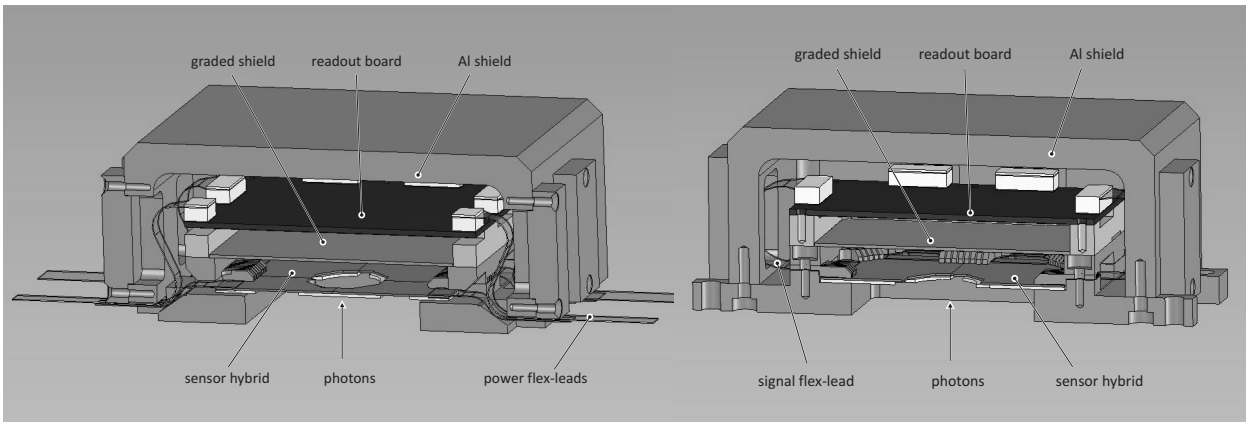

Figure 12. Two perpendicular cross sections of the HTRS sensor assembly.

SUMMARY AND OUTLOOK

The High Time Resolution Spectrometer is based on a multi-channel Silicon Drift Detector, enabling X-ray timing studies with simultaneous good energy resolution at extremely high photon rates. The SDD for the HTRS is processed in a proven and established sensor technology with a high technology readiness level. Prototype versions of the sensor and of the readout electronics will be available for a combined test within a short time.

REFERENCES

[1] http://ixo.gsfc.nasa.gov

[2] Gatti E., Rehak P., "Semiconductor drift chamber – An application of a novel charge transport scheme", *Nucl. Instr. and Meth.* **A 225** 608-614 (1984)

[3] Kemmer J.. Lutz G., "New detector concepts", *Nucl. Instr. and Meth.* **A 253** 365-377 (1987)

[4] Lechner P., Eckbauer S., Hartmann R., Krisch S., Hauff D., Richter R., Soltau H., Strüder L., Fiorini C., Gatti E. , Longoni A., Sampietro M., "Silicon drift detectors for high resolution room temperature X-ray spectroscopy", *Nucl. Instr. and Meth.* **A 377** 346-351 (1996)

[5] Pinotti E., Bräuninger H., Findeis N., Gorke H., Hauff D., Holl P., Kemmer J., Lechner P., Lutz G., Kink W., Meidinger N., Metzner G., Predehl P., Reppin C., Strüder L., Trümper J., v. Zanthier C., Kendziorra E., Staubert R., Radeka V., Rehak P., Bertuccio G., Gatti E., Longoni A., , Pullia A., Sampietro M., "The pn-CCD on-chip electronics", *Nucl. Instr. and Meth.* **A 326** 85-91 (1993)

[6] Rieder R., Gellert R., Brückner J., Klingelhöfer G., Dreibus G., Yen A., Squyres S. W., "The new Athena alpha particle X-ray spectrometer for the Mars Exploration Rovers", *Journal of Geophysical Research E: Planets* **108 (12)** ROV 7-1 - ROV 7-13 (2003)

[7] Lechner P., Buttler W., Fiorini C., Hartmann R., Kemmer J., Krause N., Leutenegger P., Longoni A., Soltau H., Stötter D., Stötter R., Strüder L., Weber U., "Multichannel silicon drift detectors for X-ray spectroscopy", *Proc. SPIE* **4012** 592-599 (2000)

[8] Fiorini C., Gola A., Longoni A., Zanchi M., Restelli A., Perotti F., Lechner P., Soltau H., Strüder L., "A large-area monolithic array of silicon drift detectors for medical imaging", *Nucl. Instr. and Meth.* **A 568** 96-100 (2006)

[9] Segneri G., Brown C., Carpenter J.-D., Kuhnle B., Lauf T., Lechner P., Lutz G., Rummel S., Strüder L., Treis J., Whitford C., "Measurement of the current related damage rate at-50°C and consequences on macropixel detector operation in space experiments", *IEEE Trans. Nucl. Sci.* **56(6)** 3734-3742 (2009)

[10] Niculae A., Lechner P., Soltau H., Lutz G., Strüder L., Fiorini C., Longoni A., "Optimized readout methods of silicon drift detectors for high-resolution X-ray spectroscopy", *Nucl. Instr. and Meth.* **A 568** 336-342 (2006)